

## Electronic Supplementary Information

### Highly efficient electrocatalytic oxidation of urea on Mn-incorporated Ni(OH)<sub>2</sub>/carbon fiber cloth for energy-saved rechargeable Zn-air battery

Xian Zhang,<sup>ab</sup> Guoqiang Liu,<sup>ab</sup> Cuijiao Zhao,<sup>ab</sup> Guozhong Wang,<sup>a</sup> Yunxia Zhang,<sup>a</sup>

Haimin Zhang<sup>\*a</sup> and Huijun Zhao<sup>ac</sup>

<sup>a</sup> Key Laboratory of Materials Physics, Centre for Environmental and Energy Nanomaterials, Anhui Key Laboratory of Nanomaterials and Nanotechnology, CAS Center for Excellence in Nanoscience, Institute of Solid State Physics, Chinese Academy of Sciences, Hefei 230031, China. E-mail: zhanghm@issp.ac.cn; Fax: +86 (0)551 65591434; Tel: +86 (0)551 65591973

<sup>b</sup> University of Science and Technology of China, Hefei 230026, China.

<sup>c</sup> Centre for Clean Environment and Energy, Griffith University, Gold Coast Campus, QLD 4222, Australia

## Experimental section

### Fabrication of Ni(OH)<sub>2</sub>/CFC, Mn-Ni(OH)<sub>2</sub>/CFC, Mn-hydroxide/CFC

**electrocatalysts.** All of the chemical reagents were analytical grade (AR) and were used without further purification. First, CFC (carbon fiber cloth, 1.0 cm×2.0 cm) was immersed in concentrated nitric acid (65 wt.%) for 48 h to adequately remove the impurity and enhance surface functional groups. Then, the CFC was rinsed with ethanol and water adequately. The Ni<sup>2+</sup>, Mn<sup>2+</sup> adsorbed CFC was obtained by immersing the pre-treated CFC in a solution containing Ni<sup>2+</sup> and Mn<sup>2+</sup> (NiCl<sub>2</sub>:MnCl<sub>2</sub>) with different molar ratios (1:0 or 2:1 or 0:1) for overnight at room temperature. The total amount of Ni<sup>2+</sup> and Mn<sup>2+</sup> in aqueous solution was 6.0 mM and the molar ratio of Ni<sup>2+</sup> to Mn<sup>2+</sup> was varied systematically. Subsequently, the as-obtained proportional Mn<sup>2+</sup>, Ni<sup>2+</sup> adsorbed CFC was immersed in a 1.0 M KOH solution to convert Mn<sup>2+</sup>,

Ni<sup>2+</sup> adsorbed CFC into Ni-Mn hydroxide/CFC. The obtained electrocatalysts in the molar ratios 1:0, 2:1 and 0:1 were denoted as Ni(OH)<sub>2</sub>/CFC, Mn-Ni(OH)<sub>2</sub>/CFC and Mn-hydroxide/CFC respectively.

Similarly, other molar ratios (Ni<sup>2+</sup>/Mn<sup>2+</sup>=1:5, 1:2, 1:1, 5:1) Ni-Mn hydroxide/CFC were prepared. The obtained electrocatalysts in the molar ratios 1:5, 1:2, 1:1 and 5:1 were denoted as Ni-Mn hydroxide/CFC-1:5, Ni-Mn hydroxide/CFC-1:2, Ni-Mn hydroxide/CFC-1:1 and Ni-Mn hydroxide/CFC-5:1, respectively.

**Fabrication of powder formed Ni-hydroxide, Mn-Ni-hydroxide and Mn-hydroxide.** The powder formed Ni-hydroxide, Mn-Ni-hydroxide and Mn-hydroxide samples were prepared by one-step solution reaction route. Firstly, the proportional Ni<sup>2+</sup>, Mn<sup>2+</sup> (NiCl<sub>2</sub>:MnCl<sub>2</sub>) solution was added into 1.0 M KOH solution under stirring for 30 min to obtain powder hydroxides. The total amount of Ni<sup>2+</sup> and Mn<sup>2+</sup> in aqueous solution was 6.0 mM and the molar ratios of Ni<sup>2+</sup> and Mn<sup>2+</sup> were 1:0, 2:1 and 0:1 respectively. After collection by filtration, washing with deionized water and freeze drying for 24 h, the powder formed powder hydroxides were obtained and denoted as Ni-hydroxide, Mn-Ni-hydroxide and Mn-hydroxide.

**Characterization.** The crystalline structures of samples were identified by X-ray diffraction analysis (XRD, Philips X'pert PRO) using Ni-filtered monochromatic CuK $\alpha$  radiation ( $\lambda_{K\alpha 1} = 1.5418 \text{ \AA}$ ) at 40 kV and 40 mA. The morphology and structure of samples were characterized by field emission scanning electron microscopy (FESEM, Quanta 200FEG) and transmission electron microscopy (TEM, JEOL 2010) with an energy dispersive X-ray spectrometer (EDS Oxford, Link ISIS).

X-ray photoelectron spectroscopy (XPS) analysis was performed on an ESCALAB 250 X-ray photoelectron spectrometer (Thermo, America) equipped with Al K $\alpha_{1,2}$  monochromatized radiation at 1486.6 eV X-ray source. Fourier transform infrared (FT-IR) spectroscopy of the sample was performed on a Perkin-Elmer TGA7 infrared spectrometer to identify the functional groups of the sample. Quantitative determination of the metal ions (Ni and Mn) content was performed by inductively coupled plasma (ICP, Thermo, America).

**Electrochemical measurements.** Electrochemical measurements were performed on an electrochemical workstation (CHI 760D, CH Instruments, Inc., Shanghai, China) coupled with a PINE rotating disk electrode (RDE) system (Pine Instruments Co. Ltd. USA). A standard three-electrode electrochemical cell equipped with gas flow system was employed during measurements. The potentials *vs.* Ag/AgCl were converted to the reversible hydrogen electrode (RHE) using the following relationship.

$$E_{\text{RHE}} = E_{\text{Ag/AgCl}} + 0.059\text{pH} + E^{\circ}_{\text{Ag/AgCl}}$$

where  $E_{\text{RHE}}$  is the converted potential *vs.* RHE,  $E^{\circ}_{\text{Ag/AgCl}} = 0.199$  V at 25°C, and  $E_{\text{Ag/AgCl}}$  is the experimentally measured potential against Ag/AgCl reference.

The UOR and OER polarization curves were measured with a scan rate of 5.0 mV s<sup>-1</sup> at room temperature in 1.0 M KOH with or without 0.5 M urea, respectively. All potentials were without *iR*-compensated. And the presented current density was normalized to the geometric surface area. All the polarization curves were the steady-state ones after several cycles. The electrochemical impedance spectroscopy (EIS)

measurements were performed by applying an AC voltage with 10 mV amplitude in a frequency range from 100,000 to 1 Hz and recorded at 1.45 V vs. RHE electrode.

*ORR measurements:* The Mn-Ni(OH)<sub>2</sub>/CFC electrode was first grinded into powder form. 4.0 mg Mn-Ni(OH)<sub>2</sub>/CFC powder catalyst was dispersed ultrasonically in 1000 μL of solvent mixture of Nafion (5%), absolute ethanol, deionized water (V: V: V=1: 1: 8), to obtain a well-dispersed catalyst ink. Subsequently, 20 μL of catalyst ink was cast onto the glassy carbon (GC) electrode surface and dried at room temperature. RDE experiments were carried out in an O<sub>2</sub>-saturated 0.1 M KOH solution at room temperature, a sweep rate of 10 mV s<sup>-1</sup> under different rotating rates (400, 625, 900, 1225 and 1600 rpm). The electron transfer number (*n*) *per* oxygen molecule at different potentials during the oxygen reduction reaction (ORR) was calculated based on the Koutecky-Levich (K-L) equation:

$$J^{-1} = J_L^{-1} + J_k^{-1} = J_K^{-1} + (B\omega^{1/2})^{-1} \quad (1)$$

$$B = 0.2nF(D_0)^{2/3}\nu^{-1/6}C_0 \quad (2)$$

$$J_k = nFkC_0 \quad (3)$$

where *J* is the measured current density, *J<sub>L</sub>* and *J<sub>K</sub>* are the diffusion- and kinetic-limiting current densities, *ω* is the rotation speed, *n* represents the number of electrons transferred *per* oxygen molecule, *F* is the Faraday constant (96485 C mol<sup>-1</sup>), *C<sub>0</sub>* is the O<sub>2</sub> concentration in the electrolyte (1.26×10<sup>-6</sup> mol cm<sup>-3</sup>), *D<sub>0</sub>* is the diffusion coefficient of O<sub>2</sub> in the electrolyte (1.9×10<sup>-5</sup> cm<sup>2</sup> s<sup>-1</sup>), and *ν* is the kinetic viscosity (0.01 cm<sup>2</sup> s<sup>-1</sup>).

*Zinc-air batteries measurement:* The measurements of Zn-air batteries were performed on home-built electrochemical cells. All data were collected from the as-fabricated cell with a Zahner-Zennium electrochemical workstation at room temperature. Briefly, Zn foil was used as anode and Mn-Ni(OH)<sub>2</sub>/CFC catalysts loaded on the gas diffusion layer was used as the air cathode. The electrolyte was 1.0 M KOH+0.2 M Zn(Ac)<sub>2</sub> with or without 0.5 M urea. The Mn-Ni(OH)<sub>2</sub> mass loading on CFC was about 0.18 mg cm<sup>-2</sup>.

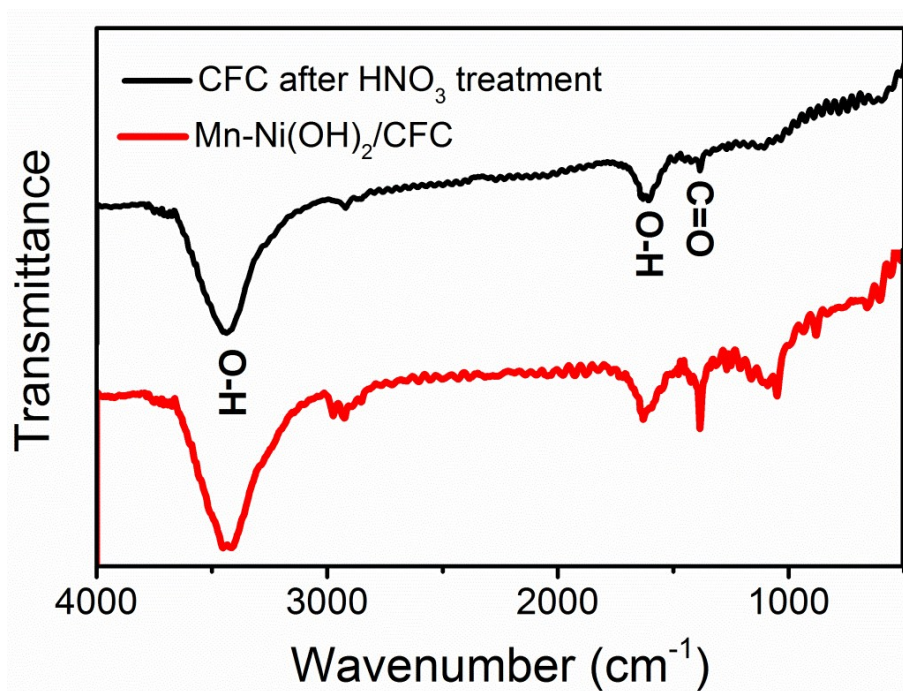


**Fig. S1** FT-IR spectrum of CFC after  $\text{HNO}_3$  treatment and  $\text{Mn-Ni(OH)}_2/\text{CFC}$

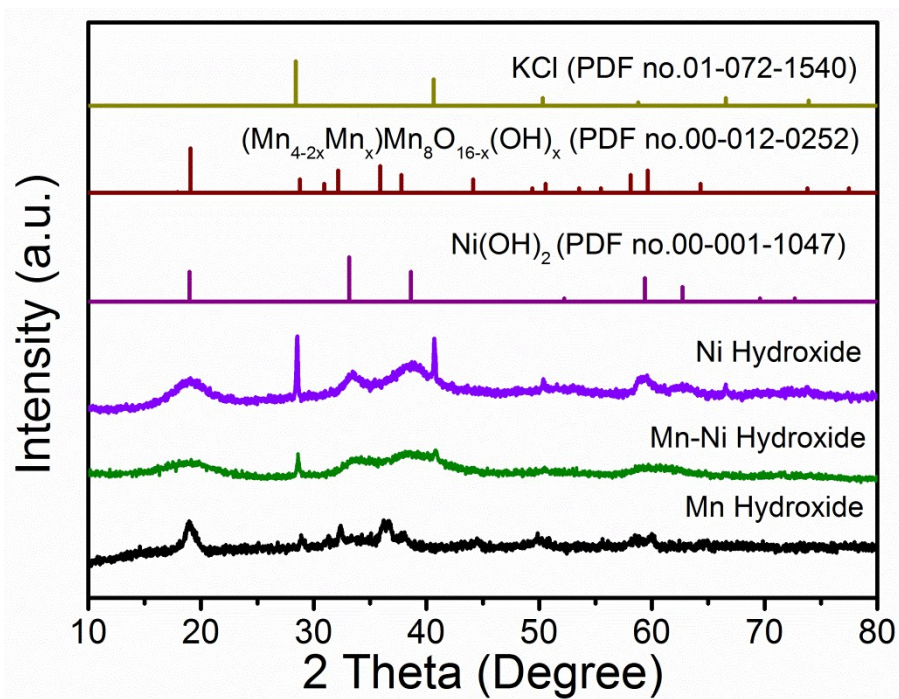


**Fig. S2** XRD patterns of powder formed Ni-hydroxide, Mn-Ni-hydroxide and Mn-hydroxide powers.

As shown in Fig. S2, pure Ni-hydroxide sample shows the diffraction peaks at 18.9°, 33.2°, 38.6°, 59.2° and 62.7°, corresponding to the (001), (100), (101), (110) and (111) crystalline planes of hexagonal Ni(OH)<sub>2</sub> (PDF no 00-001-1047), and pure Mn-hydroxide can be attributed to the (Mn<sub>4-2x</sub>Mn<sub>x</sub>)Mn<sub>8</sub>O<sub>16-x</sub>(OH)<sub>x</sub> phase (PDF no 00-012-0252), demonstrated that the Mn-Hydroxide/CFC was Mn oxyhydroxide obtained by partially dehydrated by Mn hydroxide.

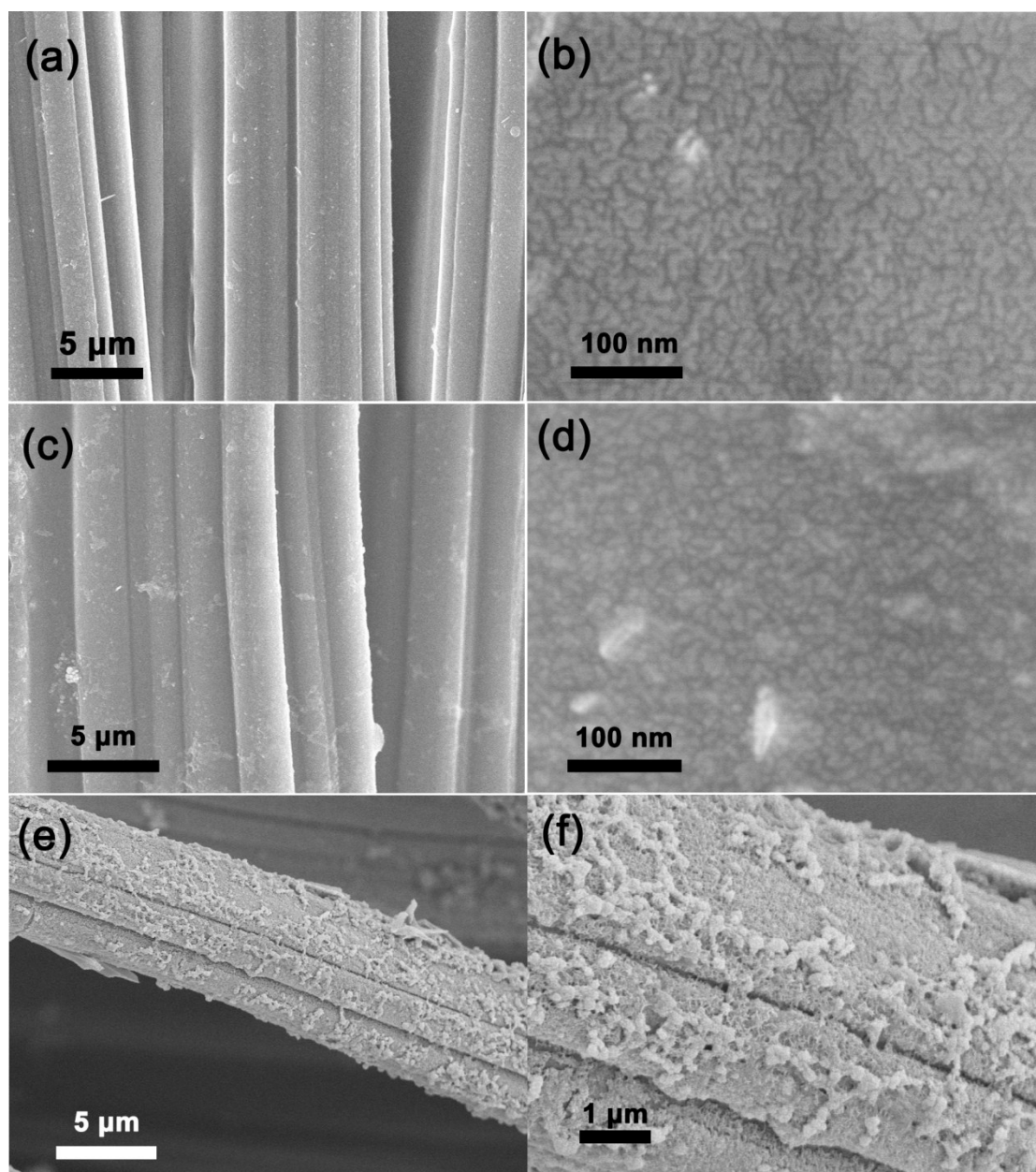


**Fig. S3** SEM images of Ni(OH)<sub>2</sub>/CFC (a), (b); Mn-Ni(OH)<sub>2</sub>/CFC (c), (d); Mn-hydroxide/CFC (e), (f).

Fig. S3 shows the surface SEM images of the as-prepared Ni(OH)<sub>2</sub>/CFC, Mn-Ni(OH)<sub>2</sub>/CFC and Mn-hydroxide/CFC samples. As shown, Ni(OH)<sub>2</sub>/CFC shows a small nanoparticle structure (Fig. S3a and b). Also, the Mn-Ni(OH)<sub>2</sub>/CFC surface presents a nanoparticle morphology adhered on the CFC surface (Fig. S3c and d);

however, Mn-hydroxide/CFC displays a characteristic nanosheet structure (Fig. S3e and f).

In our study, ICP measurements were performed to obtain the component content information of samples. The ICP results indicate that the molar ratio of Ni ( $0.13 \text{ mg cm}^{-1}$ ) to Mn ( $0.057 \text{ mg cm}^{-1}$ ) in Mn-Ni(OH)<sub>2</sub>/CFC is about 2.1:1, confirming the dominance of Ni component in sample, consistent with the results of XRD and electron microscopy characterizations.

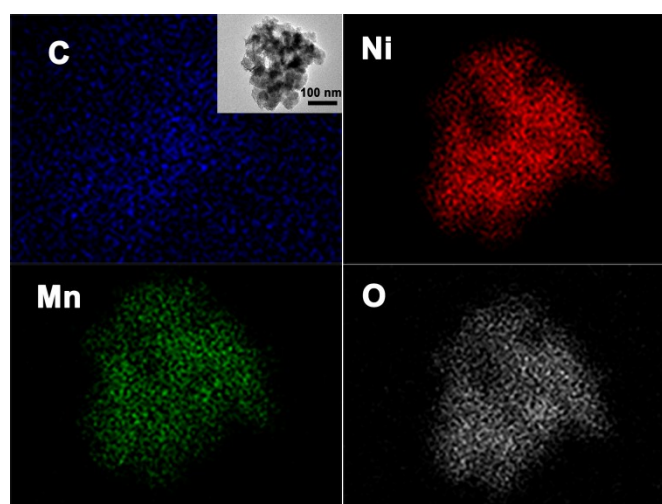


**Fig. S4** Transmission electron microscopy-energy dispersive spectroscopy (TEM-EDS) elemental mapping images of Mn-Ni(OH)<sub>2</sub>/CFC.

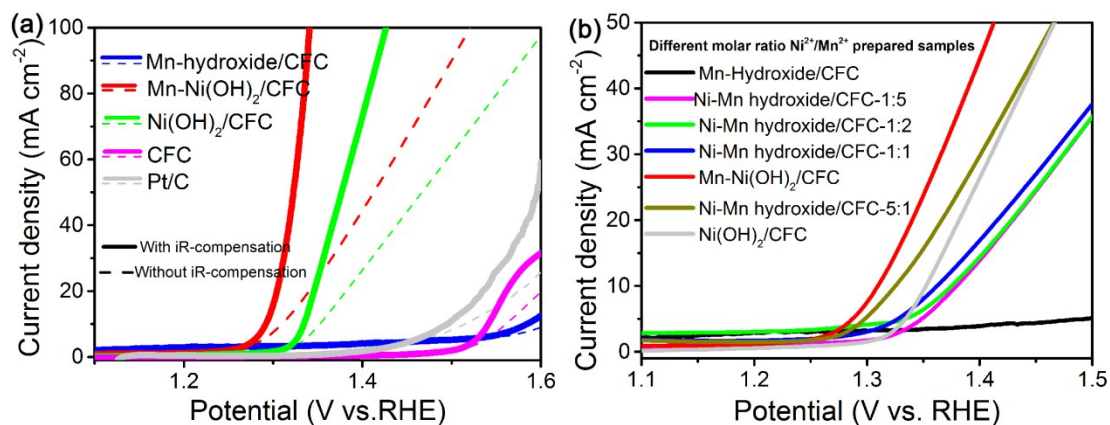


**Fig. S5** (a) UOR polarization curves with and without  $iR$  compensation of CFC, Ni(OH)<sub>2</sub>/CFC, Mn-Ni(OH)<sub>2</sub>/CFC and Mn-hydroxide/CFC in 1.0 M KOH electrolyte containing 0.5 M urea. (b) UOR polarization curves without  $iR$  compensation of different molar ratio of Ni<sup>2+</sup>/Mn<sup>2+</sup> prepared samples in 1.0 M KOH electrolyte containing 0.5 M urea.

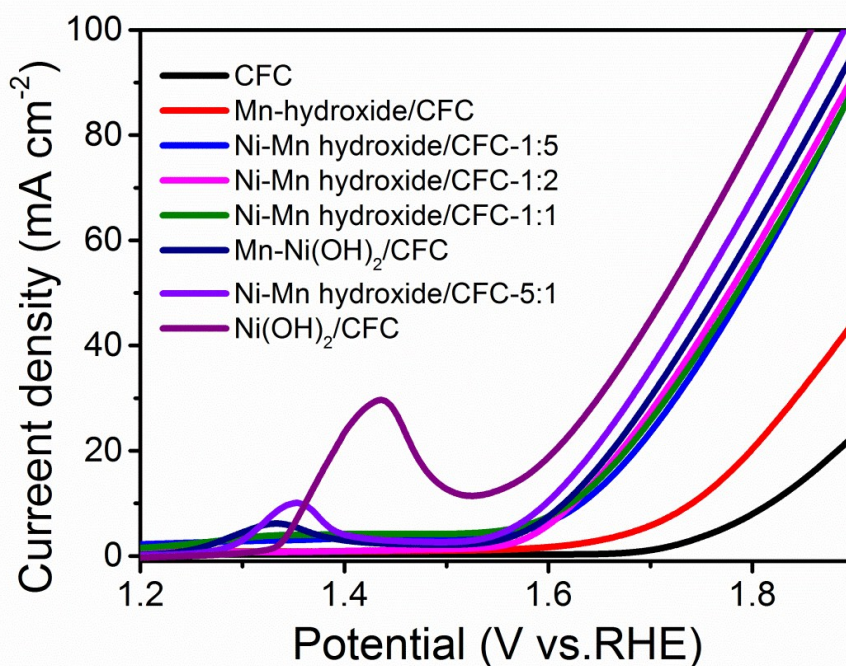


**Fig. S6** OER polarization curves without  $iR$  compensation without  $iR$  compensation of different molar ratio of Ni<sup>2+</sup>/Mn<sup>2+</sup> prepared samples in 1.0 M KOH electrolyte.

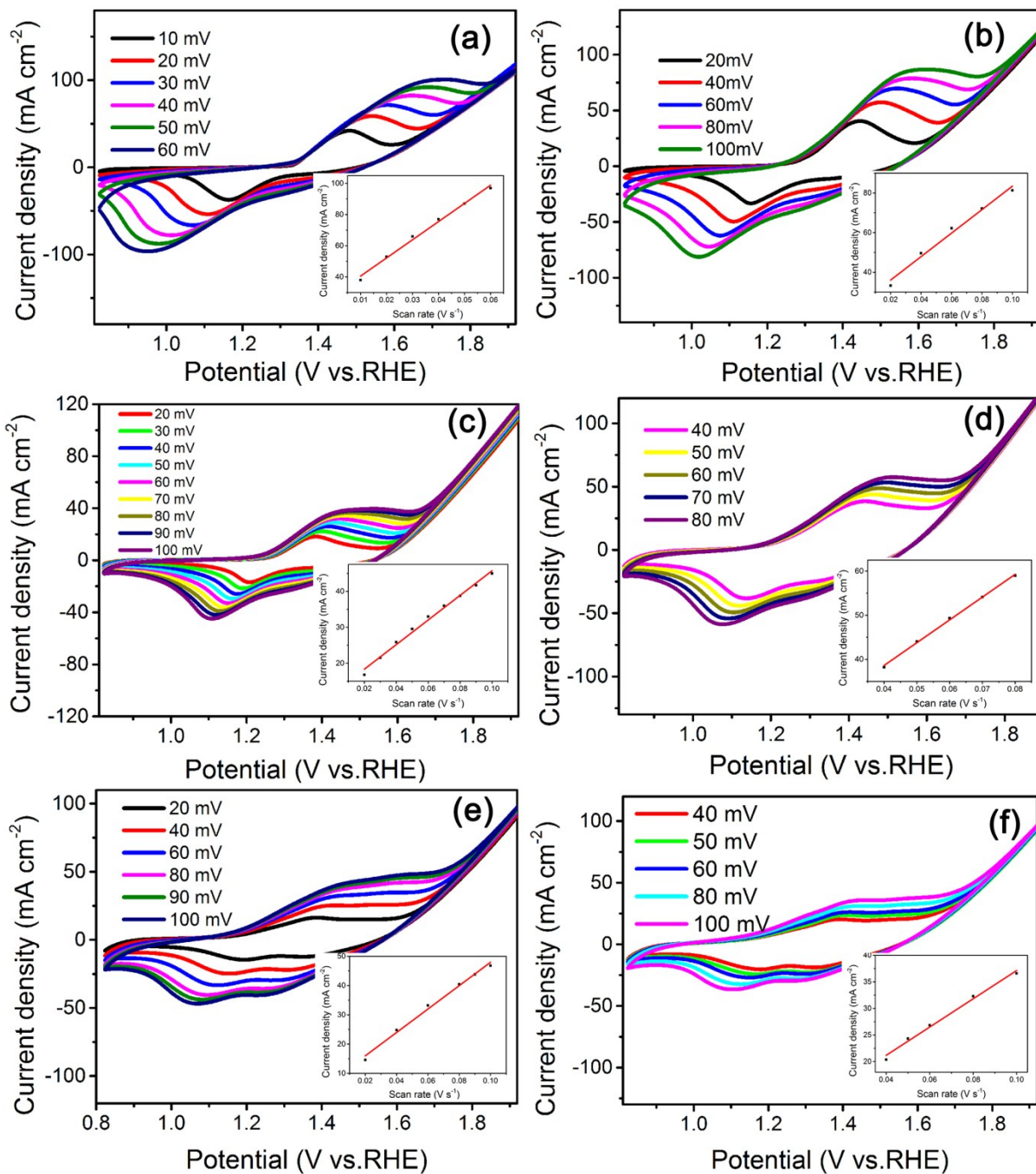


**Fig. S7.** Cyclic voltammograms of (a) Ni(OH)<sub>2</sub>/CFC, (b) Ni-Mn hydroxide/CFC-5:1, (c) Mn-Ni(OH)<sub>2</sub>/CFC, (d) Ni-Mn hydroxide/CFC-1:1 (e) Ni-Mn hydroxide/CFC-1:2, (f) Ni-Mn hydroxide/CFC-1:5.

As we known, the surface concentration of redox active Ni centers can be extracted from the slope of the linear relationship between the peak current of the Ni<sup>III</sup>/Ni<sup>II</sup>

reduction wave and the scan rate:

$$\text{slope} = n^2 F^2 A \Gamma_0 / 4RT$$

where  $n = 1$ ,  $F$  is Faraday constant ( $96485 \text{ C mol}^{-1}$ ),  $A$  is the surface area of the electrode ( $1.0 \text{ cm}^2$ ),  $\Gamma_0$  is surface concentration ( $\text{mol cm}^{-2}$ ),  $R$  is ideal gas constant ( $8.314 \text{ J mol}^{-1} \text{ K}^{-1}$ ),  $T$  is temperature ( $298 \text{ K}$ ). From the figure S8, it can be seen the  $\text{Ni(OH)}_2/\text{CFC}$  displays the largest slope value, and with the Mn content increasing, the slope value gradually decreased. Therefore it is reasonable to believe that  $\text{Ni(OH)}_2/\text{CFC}$  possesses more Ni-related catalytic active sites, thus obtaining higher OER performance in comparison with other ratio electrocatalysts.

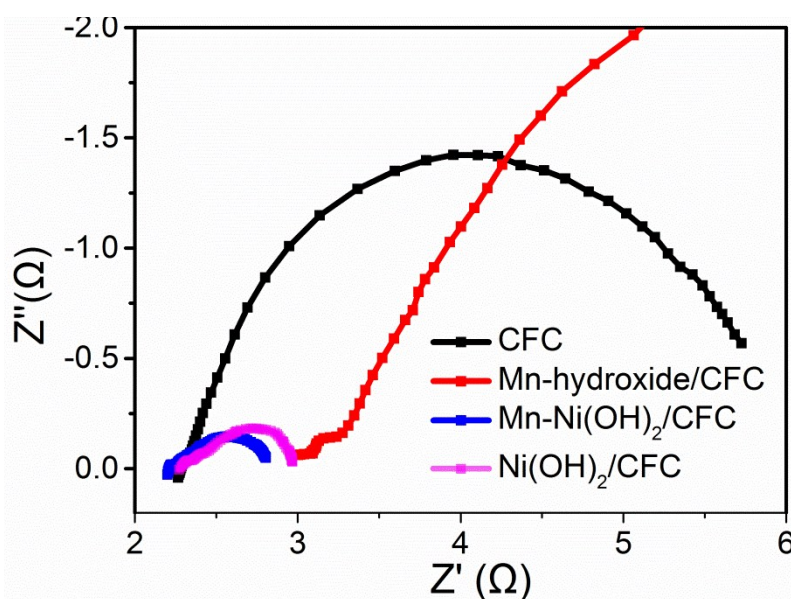


**Fig. S8** EIS of CFC,  $\text{Ni(OH)}_2/\text{CFC}$ ,  $\text{Mn-Ni(OH)}_2/\text{CFC}$  and  $\text{Mn-hydroxide}/\text{CFC}$  measured in 1.0 M KOH and 0.5 M urea electrolyte applying an AC voltage with 10 mV amplitude in a frequency range from 100,000 to 1 Hz and recorded at 1.45 V vs. RHE.

As shown in Fig. S8, the smallest series resistance ( $R_s=2.25 \Omega$ ) and charge transfer resistance ( $R_{ct}=2.75 \Omega$ ) can be achieved for Mn-Ni(OH)<sub>2</sub>/CFC, revealing its superior electrical conductivity and UOR activity by optimum Mn incorporation.

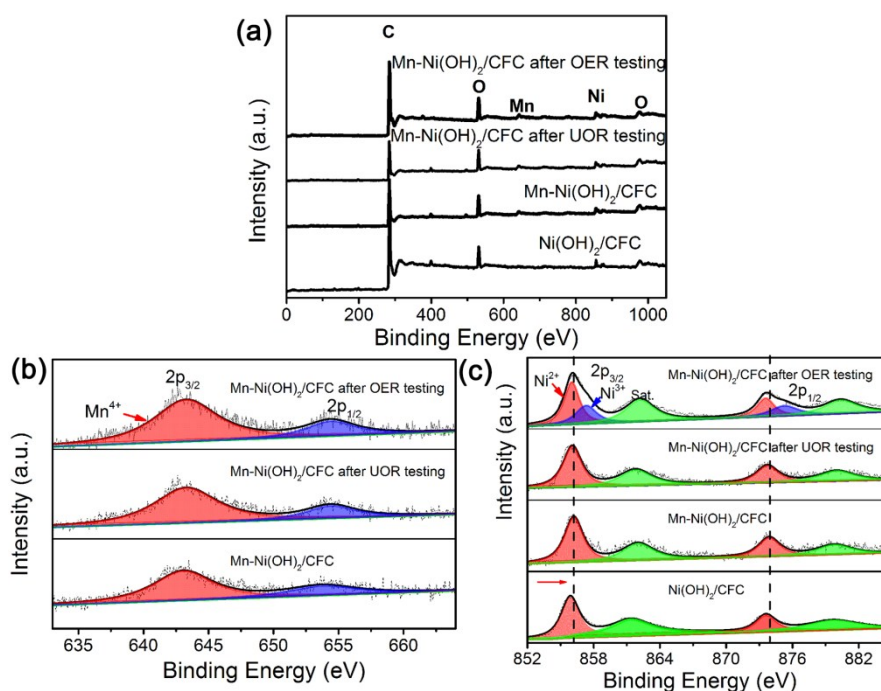


**Fig. S9** (a) XPS survey spectra of fresh Ni(OH)<sub>2</sub>/CFC, Mn-Ni(OH)<sub>2</sub>/CFC, Mn-Ni(OH)<sub>2</sub>/CFC after UOR testing and Mn-Ni(OH)<sub>2</sub>/CFC after OER testing. (b) high resolution Mn 2p XPS spectrum of fresh Mn-Ni(OH)<sub>2</sub>/CFC, Mn-Ni(OH)<sub>2</sub>/CFC after UOR testing and Mn-Ni(OH)<sub>2</sub>/CFC after OER testing. (c) high resolution Ni 2p XPS spectrum of fresh Ni(OH)<sub>2</sub>/CFC, Mn-Ni(OH)<sub>2</sub>/CFC, Mn-Ni(OH)<sub>2</sub>/CFC after UOR testing and Mn-Ni(OH)<sub>2</sub>/CFC after OER testing.

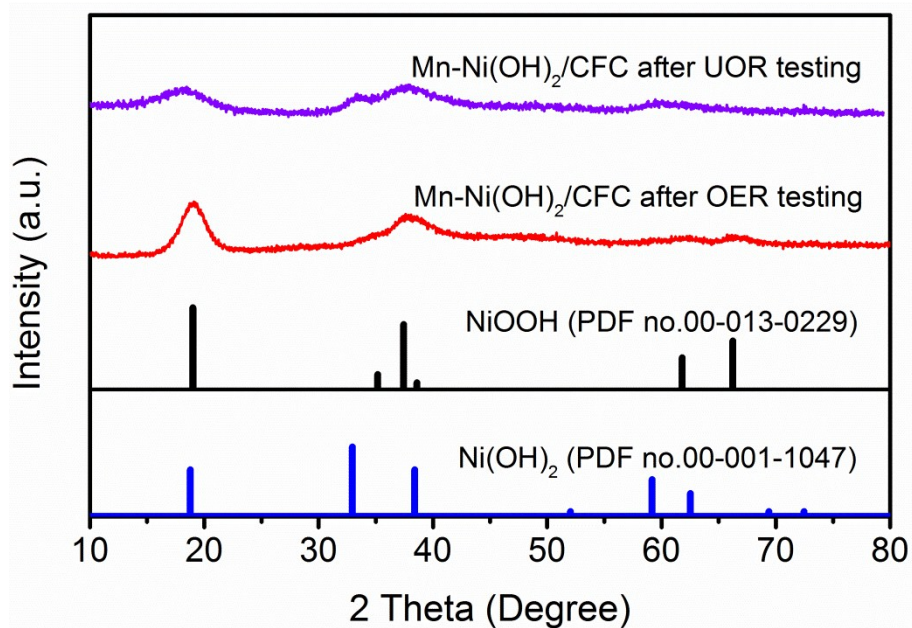


**Fig. S10** XRD patterns of powder Mn-Ni(OH)<sub>2</sub> after OER/UOR testing.

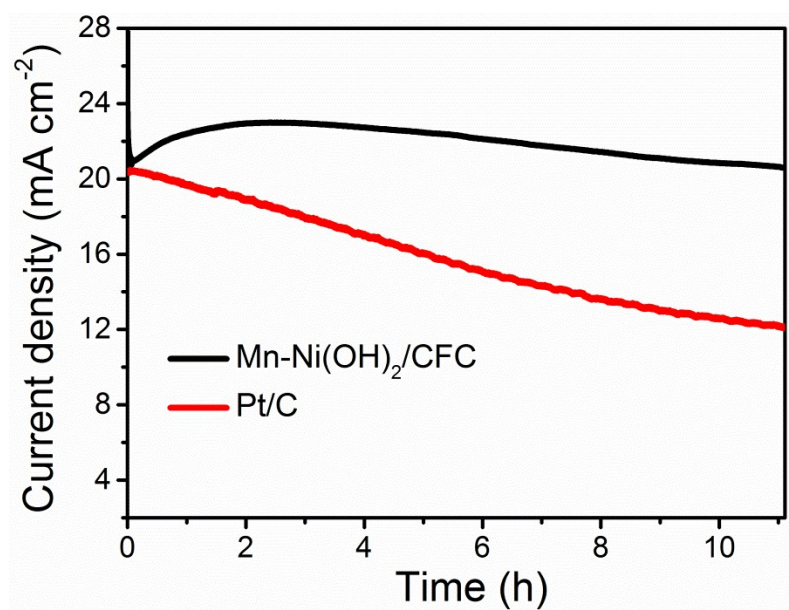


**Fig. S11** Durability test for the Mn-Ni(OH)<sub>2</sub>/CFC and Pt/C samples in 1.0 M KOH solution with 0.5 M urea.

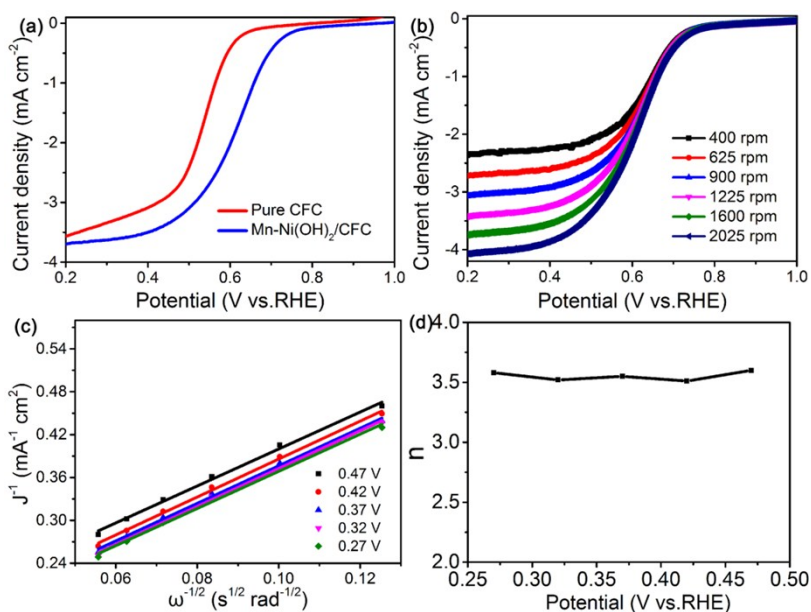


**Fig. S12** (a) LSV curves of, pure CFC and Mn-Ni(OH)<sub>2</sub>/CFC in O<sub>2</sub>-saturated 0.1 M KOH solution at a scan rate of 10 mV s<sup>-1</sup> and a rotation speed of 1600 rpm, (b) LSV curves of Mn-Ni(OH)<sub>2</sub>/CFC obtained at different rotating rates in O<sub>2</sub>-saturated 0.1 M KOH solution at a scan rate of 10 mV s<sup>-1</sup>, (d) Koutecky-Levich (K-L) plots of Mn-Ni(OH)<sub>2</sub>/CFC derived from (b), (d) electron transfer number (n).

The ORR activity of Mn-Ni(OH)<sub>2</sub>/CFC was therefore evaluated in 0.1 M KOH with a PINE rotating disk electrode (RDE) system. The LSV curves of Mn-Ni(OH)<sub>2</sub>/CFC obtained from an O<sub>2</sub>-saturated 0.1 M KOH solution at different rotation rates are shown in Fig. S12b. As shown, the investigated electrocatalyst exhibits the onset potential of ca. 0.83 V (vs. RHE), and the limiting current density increases with the rotation rate. Based on Fig. S12b, the derived Koutecky–Levich (K-L) plots are shown in Fig. S12c, exhibiting a good linear relationship. On the basis of the K–L plots, the average value of the number of transferred electrons (Fig. S12d) within 0.27-0.47 V (vs. RHE) was calculated to be 3.7 for Mn-Ni(OH)<sub>2</sub>/CFC, indicating a near four electron ORR process.

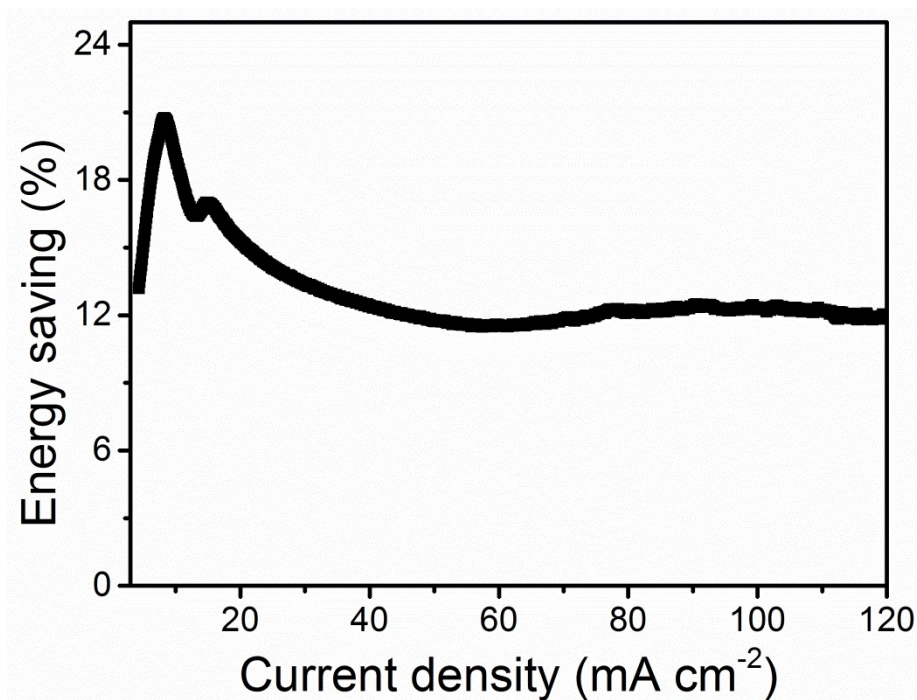


**Fig. S13** The charging energy saving efficiency curves of Zn-air battery with 0.5 M urea.

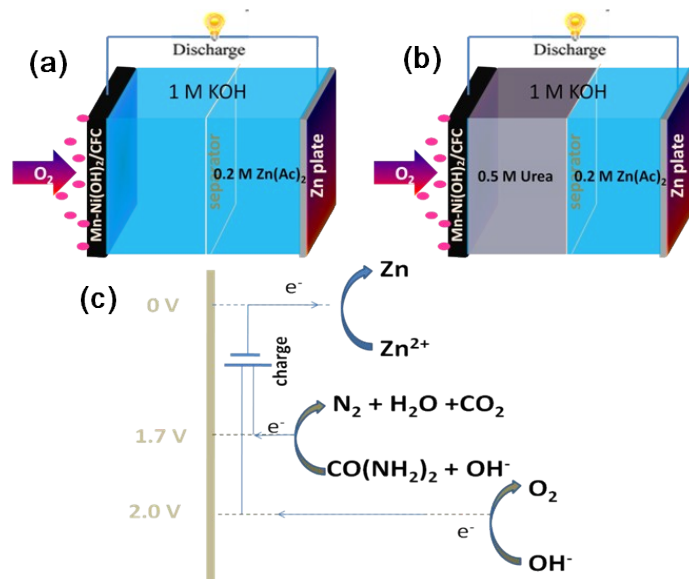


**Fig. S14** (a) The Zn-air battery assembled by Mn-Ni(OH)<sub>2</sub>/CFC as air cathode. (b) The urea-assisted charging Zn-air battery assembled by Mn-Ni(OH)<sub>2</sub>/CFC as air cathode. (c) In charging process, the charging voltage of a rechargeable Zn-air battery is compensated by the potential difference between oxidation of urea and water.

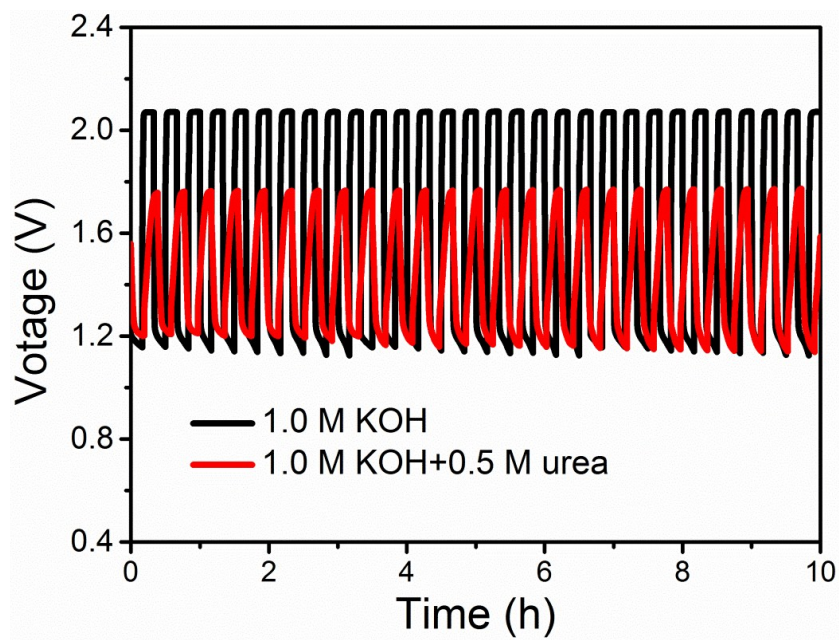


**Fig. S15** Recycling durability test of home-made rechargeable Zn-air battery.

**Table S1.** Comparison of the UOR activities for recently reported highly active electrocatalysts.

References	Catalyst	Potential at 10 mA cm <sup>-2</sup> (V vs. RHE)	Mass loading (mg cm <sup>-1</sup> )	Electrolyte
<i>Angew. Chem., 2016, 128, 3868</i>	S-MnO <sub>2</sub>	1.33	1.5	1 M KOH + 0.5 M Urea
<i>Chem. Commun., 2009, 32, 4859</i>	Pt	1.50	2.5	5 M KOH + 0.33 M Urea
<i>Angew. Chem. Int. Ed., 2016, 55, 12465</i>	M-Ni(OH) <sub>2</sub>	1.38	0.535	1 M KOH + 0.33 M Urea
<i>J. Power Sources, 2014, 272, 711</i>	NiO nanosheet array	1.38	0.27	1 M KOH + 0.33 M Urea
<i>Electrochim. Acta, 2015, 153, 456</i>	NiMo sheet array	1.37	0.35	1 M KOH + 0.33 M Urea
<i>Sci. Rep., 2014, 4, 5863</i>	NiCo alloy	1.53	10	1 M KOH + 0.33 M Urea
<b>This work</b>	<b>Mn-Ni(OH)<sub>2</sub>/CFC</b>	<b>1.30</b>	<b>0.18</b>	<b>1 M KOH + 0.5 M Urea</b>